

Application of Photogrammetric 3D Reconstruction to Scanning Electron Microscopy: Considerations for Volume Analysis

William D. A. Rickard

John de Laeter Centre, Curtin University, Bentley, WA, 6102, Australia
E-mail: W.Rickard@curtin.edu.au

Jéssica Fernanda Ramos Coelho

John de Laeter Centre, Curtin University, Bentley, WA, 6102, Australia
Curtin HIVE, Curtin University, Bentley, WA, 6102, Australia

Joshua Hollick, Susannah Soon, and Andrew Woods[▲]

Curtin HIVE, Curtin University, Bentley, WA, 6102, Australia

Abstract. Photogrammetric three-dimensional (3D) reconstruction is an image processing technique used to develop digital 3D models from a series of two-dimensional images. This technique is commonly applied to optical photography though it can also be applied to microscopic imaging techniques such as scanning electron microscopy (SEM). The authors propose a method for the application of photogrammetry techniques to SEM micrographs in order to develop 3D models suitable for volumetric analysis. SEM operating parameters for image acquisition are explored and the relative effects discussed. This study considered a variety of microscopic samples, differing in size, geometry and composition, and found that optimal operating parameters vary with sample geometry. Evaluation of reconstructed 3D models suggests that the quality of the models strongly determines the accuracy of the volumetric measurements obtainable. In particular, they report on volumetric results achieved from a laser ablation pit and discuss considerations for data acquisition routines. © 2020 Society for Imaging Science and Technology.

[DOI: 10.2352/J.ImagingSci.Technol.2020.64.6.060404]

1. INTRODUCTION

A scanning electron microscope (SEM) scans a focused electron beam over the surface of a sample under high vacuum to produce an image (micrograph) [1]. Spatial resolution down to 1 nm is achievable [2] and there are a number of detectable signals that reveal a wealth of information, including sample morphology and composition. Additional information can be derived by converting the two-dimensional (2D) micrographs into a digital three dimensional (3D) model of the sample [3].

Three-dimensional analysis of microscopic surfaces can be achieved by atomic force microscopy [4], optical profilometry [5], and a number of other analytical techniques.

[▲] IS&T Member.

Received July 16, 2020; accepted for publication Nov. 5, 2020; published online Dec. 30, 2020. Associate Editor: Henry Y.T. Ngan.

1062-3701/2020/64(6)/060404/9/\$25.00

However, these techniques require a dedicated instrument and have limited field of view and depth of field when compared to SEM. A more efficient workflow can be achieved by creating the 3D model from data collected during 2D surface analyses in SEM. Shape from Shading (SFS) [6, 7] or collecting stereo-pair images are techniques that have been applied to SEM micrographs for 3D reconstructions. Recently, photogrammetric 3D reconstruction has been proposed as a potential method for 3D reconstruction of SEM micrographs, with a number of advantages over other techniques [8–11].

Photogrammetry is a method for extracting three-dimensional coordinates from a group of 2D photographs [12]. Photogrammetric 3D reconstruction combines photogrammetry with computer vision and image processing techniques to calculate detailed digital 3D models with arbitrary complexity from an often large collection of 2D photographs. The technique involves a multistage process comprising (a) feature extraction, (b) feature matching, (c) bundle adjustment, (d) coarse point cloud generation, (e) dense point cloud generation, (f) mesh generation from the point cloud, and finally (g) texturing the mesh [13–15]. The resultant digital 3D model can be highly detailed and visually accurate [16–18]. The complexity of the model and the size of the texture file can be customized depending upon the requirements of the user. There are many advantages of having an accurate 3D model of a microscopic object of interest including the ability to more accurately assess the shape of an item and the potential to conduct 3D measurements of the item including surface area and volume. Digital 3D models also have the advantage that they can be used to create virtual reality and augmented reality experiences—allowing people to experience the items as if they were real-world objects at much larger size. The models can also be used in animation packages (such as POVray or Blender) to create animated video sequences of the item from arbitrary angles or paths.

Volumetric analysis of microscopic samples is of significant interest as it can be used for quantitative measurements of things such as particle volume, pore volume, and surface area. One application of particular interest is the analysis of the volume of laser ablation (LA) sputter pits, where the volume measurements are used to facilitate quantitative chemical/isotopic concentration analyses by inductively coupled plasma mass spectrometry (ICP-MS) [19]. Simple volume measurements can be made by fitting a defined shape (e.g. cylinder, sphere) to the object/void and measuring its dimensions to calculate the volume. However, objects/voids of irregular shapes cannot be accurately measured in this way.

There are a few published examples of the application of photogrammetry to SEM, with the purpose of 3D visualization. Khokhlov et al. [20] used photogrammetry to study 3D fractures and surface roughness in microstructures and Amish et al. [8] used the technique to reconstruct an Ebola virus infected cell for visualization. Ball et al. [18] developed a process using macros for automated SEM stage movement and imaging to optimize micrograph acquisition for 3D reconstruction using a variety of samples, imaging platforms, and reconstruction programs. Eulitz and Reiss [10], who used photogrammetry to reconstruct a rabbit kidney glomerulus, reported optimal stage rotation increments of 9° and used manual stitching of the micrographs due to inaccuracies associated with the “virtual circle” (ring of modeled camera positions around the sample). Verification was done by superimposing a micrograph onto the corresponding image in the 3D reconstruction.

A number of recent studies have extended the 3D visualization to include quantitative measurements. It has been demonstrated that photogrammetric reconstructions from SEM images can be used for quantitative surface measurements including surface roughness, geometrical measurements, and surface topography [21–24]. The application of SEM photogrammetric models to volume measurement had been limited. Masson et al. [11] compared volume measurements of gold particles by X-ray microscopy and SEM photogrammetry. The study used one data collection method (stage tilt 70° , image rotation 18° , 20 images) and found that the error between the methods was between 6% and 43%, depending on the size of the particle and the completeness of the reconstruction.

In this contribution, we extend the utility of SEM micrographs by proposing a methodology for an efficient photogrammetric approach to understanding the 3D shape of microscopic objects. The work contributes by improving existing data acquisition processes for photogrammetry and providing a basis for accurate quantitative volume measurements. These measurements are useful in a wide range of research areas including cell volume and biostructure measurements in biology, crystal and pore size in materials science, and volume and surface thickness of drug delivery microcapsules in pharmacology.

In this article, results from two distinct data collection methods are presented using three sample types. A comparative volume analysis is conducted on synthetic and irregular

laser pits. The discussion and conclusion sections summarize the findings and implications of the study.

2. METHODS

Microscopic samples were selected for their geometric and compositional differences. Laser ablation pits in a quartz mineral substrate were used to evaluate the photogrammetric analysis of pores/voids. A synthetic laser ablation pit with a cylindrical shape was milled into a silicon substrate and used for the volume analysis experiment. Zircon (ZrSiO_4) crystals and a drug delivery microcapsule were used to evaluate the photogrammetric analysis of particles. The samples were mounted onto an aluminum stub and coated with 3 nm platinum coating to make them conductive for SEM analysis. The SEM used in this study was a Tescan Lyra3 with a field emission electron source located in the John de Laeter Centre at Curtin University, Western Australia.

Photogrammetry is conventionally performed using optical cameras to capture multiple images of objects from different perspectives. Here, we followed a similar process using the SEM to acquire multiple micrographs from different stage positions relative to the incident electron beam. The series of micrographs were acquired from different rotations and tilt angles by adjusting the high precision, five axis, compucentric sample stage in the SEM.

This study carefully evaluated the influence of the most significant operating parameters: stage tilt and stage rotation. Other SEM operating parameters such as accelerating voltage, scan speed, magnification, and working distance were sample dependant and not specific to the photogrammetric data analysis process. The accelerating voltage was set to 5 kV for delicate samples and 10 kV for others. Working distances (WDs) were between 8 mm and 18 mm, with the longer WDs better for a greater depth of field in larger samples. Magnification was set to ensure the field of view covered the entire sample in each micrograph. Electron beam scan speeds of 4 s/frame ($3.2 \mu\text{s}/\text{pix}$), 21.5 s/frame ($10 \mu\text{s}/\text{pix}$), and 43 s/frame ($32 \mu\text{s}/\text{pix}$) were used, with a time versus quality trade-off. For example, sufficient quality micrographs of the zircon crystals were acquired at a scan speed of 43 s/frame ($32 \mu\text{s}/\text{pix}$), whereas a scan speed of 4s/frame ($3.2 \mu\text{s}/\text{pix}$) was sufficient for the laser pits. Secondary electrons (SE) were collected using the Everhart–Thornley detector (off-axis SE) and the In-beam detector (axial SE). The backscattered electron (BSE) detector was used for the zircon sample for atomic number contrast.

In Table I, we describe two methods in which we study stage tilt and rotation. **Method 1** - Variable stage tilt: micrographs were acquired with a stage tilt ranging from -15° to $+35^\circ$ at 2.5° tilt intervals (off-axis SE) or -25° to $+70^\circ$ (axial SE), at intervals of 2.5° or 5° , combined with a manual stage rotation of 0° , 45° and 90° . **Method 2** - Fixed stage tilt combined with manual stage rotation: the sample stage was fixed at a tilt of 45° and an images series was collected using manual stage rotation through 360° at 5° intervals. Illustrations of the camera locations for each of the methods are in the supplementary data.

Table I. Summary of the main SEM working parameters for data collection. For Method 1: Automated Stage Tilt: Values of stage rotation were fixed, micrographs were acquired by automatically tilting the sample stage. For Method 2: Fixed Stage Tilt and Manual Stage Rotation: Values of stage tilt were fixed, micrographs were acquired by rotating the sample stage.

	Detector	Scan speed	Stage tilt (°)	Stage rotation (°)	Increment (°)	No. of micrographs	Total images	Acquisition time (min)
Method 1	Off-axis SE	4 s/frame (3.2 μ s/pix)	-15 to +35	0	2.5	20	60	15
	Off-axis SE	4 s/frame (3.2 μ s/pix)	-15 to +35	45	2.5	20		
	Off-axis SE	4 s/frame (3.2 μ s/pix)	-15 to +35	90	2.5	20		
	Axial SE	4 s/frame (3.2 μ s/pix)	-25 to +70	0	5	19	57	15
	Axial SE	4 s/frame (3.2 μ s/pix)	-25 to +70	45	5	19		
	Axial SE	4 s/frame (3.2 μ s/pix)	-25 to +70	90	5	19		
Method 2	Axial SE	43 s/frame (32 μ /pix)	45	0 to 360	5	72	72	60
	BSE	43 s/frame (32 μ /pix)	45	0 to 360	5	72	72	60

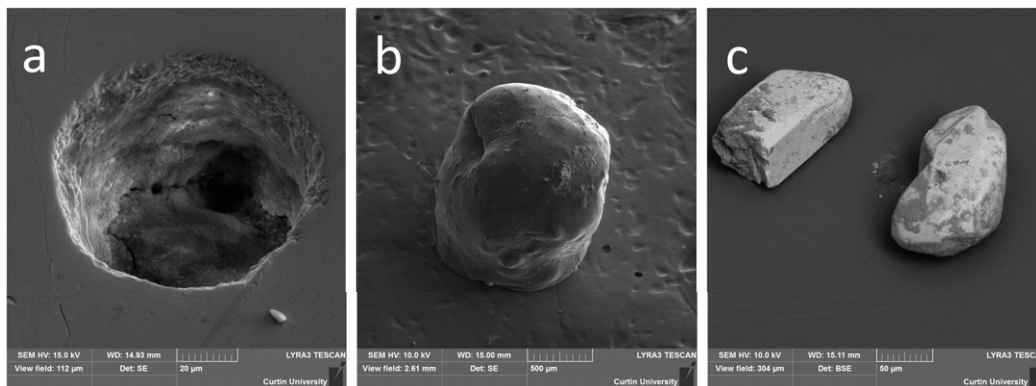


Figure 1. SEM micrographs of the samples used in this study. (a) irregular laser pit, (b) drug delivery microcapsule, and (c) zircon crystals.

Micrographs were collected using the two methods for the laser pit, zircon, and microcapsule samples (Figure 1). Electron column settings related to the aperture angle, where the imaging is optimized for resolution or depth, were also varied in trials. Table II summarizes the most time-effective operating parameters for 3D reconstruction of the three samples.

Photogrammetric data analysis was performed using the software Agisoft PhotoScan Professional (Agisoft PhotoScan, Version 1.4.1)—recently renamed Agisoft Metashape. PhotoScan was chosen for its better performance compared to other programs used for 3D reconstruction from micrographs [9], simple workflow, variety of model visualization options (including point clouds and textured meshes), and linear and surface area measurement functions. The SEM images were aligned by the Agisoft PhotoScan software using a feature recognition algorithm (further details in Gruen et al. [25] and references therein) to create a point cloud and a set of camera positions relative to the sample. Volume measurements of 3D models were conducted using the PhotoScan function “Measure Area and Volume”.

3. RESULTS

3.1 Generating 3D Models from Various Microscopic Sample Types

Successful photogrammetric reconstructions were derived from micrographs that were captured using a range of detectors (axial SE, off-axis SE, and BSE), each with different signal intensities and contrast mechanisms. Images that negatively influenced alignment (e.g. out of focus or brightness/contrast not matching other images) were manually removed. Over 50 unique point cloud reconstructions of samples were generated in this study using PhotoScan. The micrographs for each sample were aligned to build a sparse point-cloud, dense point-cloud, and mesh models. Texture and tiled models were then built. Reconstruction was successful when micrographs with matching features from consistently overlapping images were included in the dataset.

Micrographs for the photogrammetric reconstruction of the irregular laser pit (Fig. 1a) were collected using Method 1 (variable stage tilt and rotation) and the axial SE detector, taking approximately 15 minutes to collect (Figure 2). Method 2 was also effective for the reconstruction of this laser pit. However, the time required for data collection

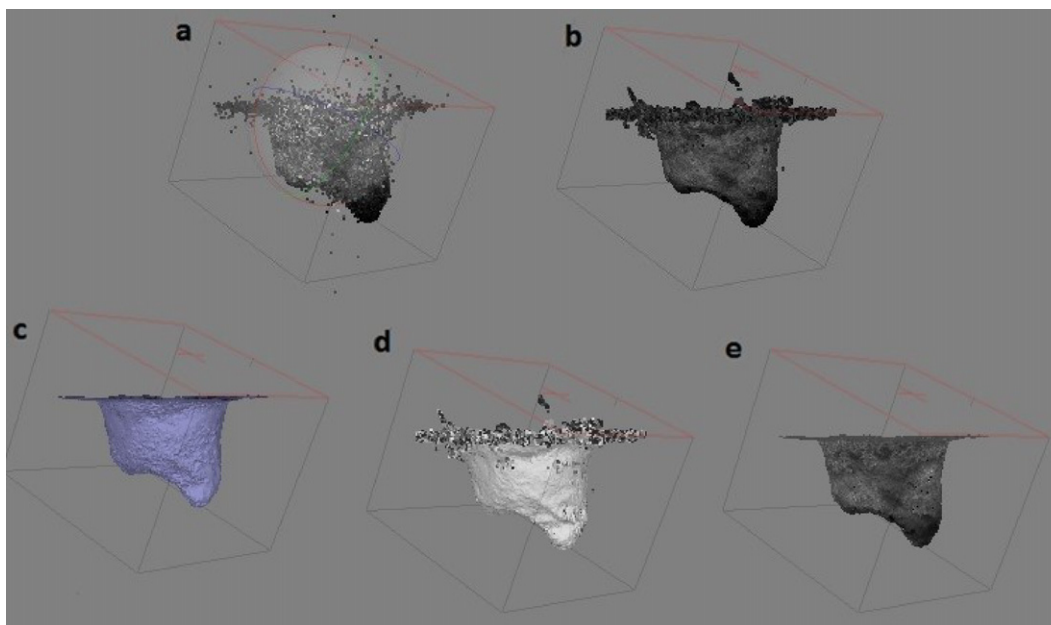


Figure 2. 3D model reconstruction of an irregular laser pit using PhotoScan. (a) point cloud, (b) dense cloud, (c) wireframe, (d) solid view, and (e) textured model.

Table II. Optimal SEM working parameters for data collection of a laser pit, microcapsule, and zircon crystals. AccV: Accelerating Voltage; Mag: Magnification; SS: Scan Speed.

Method	Sample	AccV (kV)	WD (mm)	Mag (x)	SS	Stage tilt (°)	Stage rotation (°)	Stage rotation increment (°)	No. of micrographs	Time (min)
1	Irregular laser pit	10	15	700	4 s/frame (3.2 μ s/pix)	-25 to +70	0, 45, and 90	5	57	15
2	Microcapsule	5	14	133	21.5 s/frame (32 μ s/pix)	45	0 to 360	5	72	60
3	Zircon	10	10	910	43 s/frame (32 μ s/pix)	45	0 to 360	5	72	60

was significantly longer (60 minutes versus 15 minutes with Method 1).

The photogrammetric reconstructions for the microcapsule are shown in Figure 3. Data were collected using Method 2 (fixed stage tilt) with off-axis SE imaging and took approximately 60 minutes to collect. The off-axis SE detector resulted in non-uniform illumination of the sample and some shadowing though had the advantage of high signal and high resolution (Fig. 1b).

The 3D model for the zircon crystals sample is shown in Figure 4. The data was collected using Method 2 (fixed stage tilt) and BSE imaging and took approximately 60 minutes to collect (details for the reconstruction of all three samples in Table II). An advantage of the use of a BSE detector is the atomic number contrast in the images allows the differentiation of the bright zircon crystal and the dark contamination on the surface. A disadvantage of the BSE detector was that the low signal intensity required a slow scan rate (43 s/frame), requiring more time to collect each micrograph.

A stereoscopic 3D video of the microcapsule and zircons is available via a link in the supplementary data.

In Method 1, the angle of the stage tilt varied whilst micrographs were acquired from three different stage rotation angles. This allowed samples to be completely visualized from a top down view, for example, enabling the concave laser pit to be successfully 3D reconstructed. An advantage of Method 1 is that the stage tilt angle increment can be specified to optimize the number of micrographs required for a 3D reconstruction so that there are sufficient micrographs to maintain overlap between images and have common features in neighboring micrographs for feature matching to occur. It was found that a minimum dataset for the irregular laser pits modeled with this method can be acquired by rotating the stage only once for a stage tilt over a specified range. PhotoScan was able to reconstruct the 3D model aligning only two (for example, 40 micrographs collected at 0° and 45°) of the three (0°, 45°, and 90°, 60 micrographs) datasets. However, considering all three angles of stage rotation lead to more detailed wireframes, hence more detailed models, without relevant time differences in micrograph collection. PhotoScan was not able to reconstruct beyond the point-cloud model of this

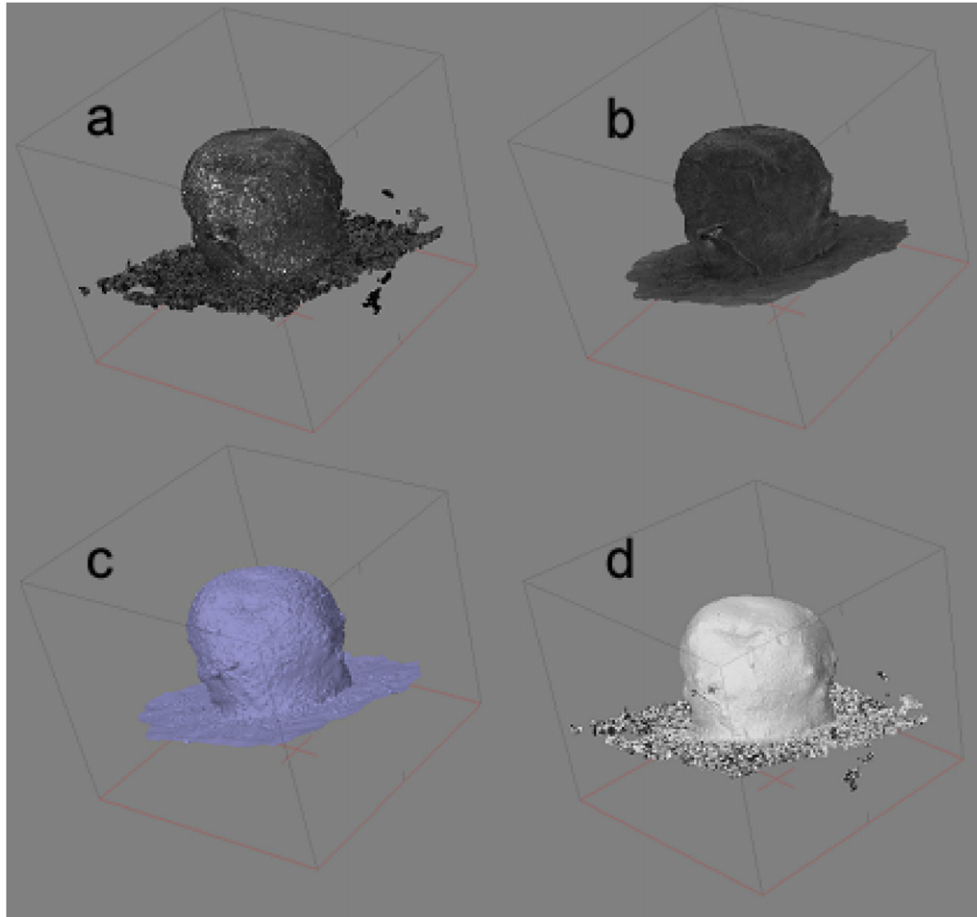


Figure 3. 3D model reconstruction of a drug delivery microcapsule using PhotoScan. (a) dense cloud, (b) textured model, (c) wireframe, and (d) solid view.

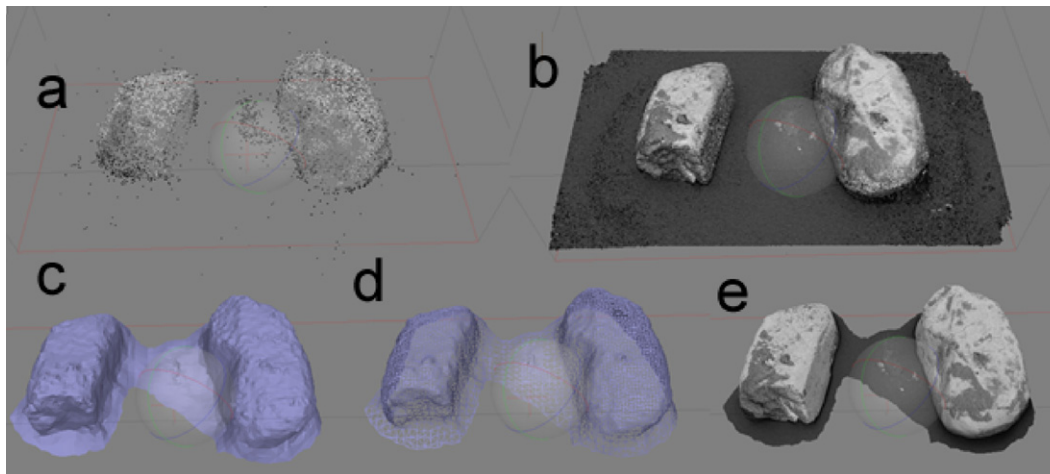


Figure 4. 3D model reconstruction of two zircon crystals using PhotoScan. (a) point cloud, (b) textured model, (c) dense wireframe, (d) wireframe, and (e) tiled model.

sample when only one dataset was aligned. Method 1 was time efficient as it was semi-automated.

Method 2 was suitable for elevated samples such as the zircon crystals and microcapsules. A complete visualization

of all sides of the sample was acquired by a 360° rotation of the sample. Method 2 can capture low angles which Method 1 may omit. Method 1 led to failed 3D models of these two samples, as the process cannot capture information from

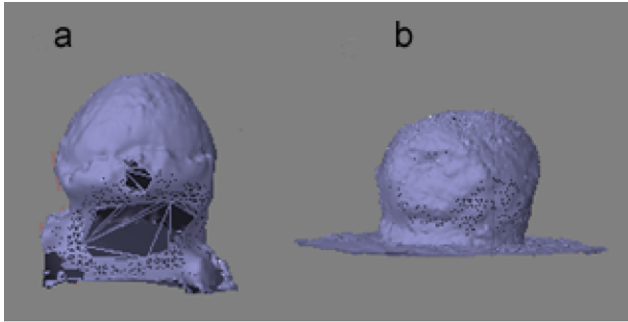


Figure 5. Wireframe models of a microcapsule reconstructed using PhotoScan with micrographs acquired (a) using Method 1: variable stage tilt; and (b) Method 2: fixed stage tilt combined with manual stage rotation. The gaps present in (a) demonstrate that Method 1 does not provide sufficient data to 3D reconstruct this elevated sample.

edges in the sample side opposing the detector (e.g. Figure 5). Method 1 was also limited by the range of automated stage tilt which is restricted to avoid the possibility of sample or microscope damage.

Other disadvantages of Method 1 included the reduced ability to control conditions such as brightness and contrast due to increased signal at higher tilt angles caused by the sample being inclined toward the detector. In addition, some undesirable defocusing was observed when the sample working distance changed slightly during tilting. A computerized stage was used though there some misalignment is inevitable when tilting through a large angle range and as such automated acquisition is negatively affected by focal length changes and the sample moving out of the field of view.

In Method 2, experimental results found that the optimal stage tilt value was 45° , also confirmed by Amish et al. [8] because lower values of state tilt failed to acquire information from margin areas between the sample and the SEM stage. Problems encountered regarding brightness, contrast, and defocusing experienced in Method 1 are reduced in Method 2, where brightness/contrast and focus can be manually adjusted for every micrograph.

3.2 Volumetric Analysis

Volume of objects in an image can be calculated by measuring the dimensions and using suitable mathematical equations. Alternatively, using photogrammetric models, volume can be derived from the model, requiring only the setting of the scale of the 3D model by manual specification of a point–point distance measurement. To compare volume analysis measurement, we analyzed both an irregular laser pit and a synthetic laser pit.

Synthetic laser pit: We first considered a regular shaped, symmetrical and smooth synthetic silicon laser pit (Figure 6). The volume of this microscopic sample was calculated using measurements from 2D image analysis and photogrammetry.

For SEM volume measurements, volume was calculated using depth and radius measurements from the micrographs in Fig. 6, with the approximation that synthetic laser pit was cylindrical. The advantage in this approach is

that only the dimensions of the shapes are required. The laser pit was calculated to have a volume of $558.61 \mu\text{m}^3$ ($5.59 \times 10^{-16} \text{m}^3$) by this method.

For photogrammetry volume measurements, volume would normally be calculated using PhotoScan's Scale Bar function over points on the 3D reconstructed model. However, the difficulty in generating a useful 3D model of the regular laser pit was observed where the featureless surface resulted in a poor 3D model result, therefore no volume calculations using this technique were obtained for comparison.

Irregular shaped laser pit: A similar test was conducted for the textured laser pit (Fig. 1a). The irregular shape meant there was no matching shape for precise volume calculation though a hemispherical shape was found to be the closed approximation. The diameter of the pit was measured to be $87.37 \mu\text{m}$ (Figure 7a), and the corresponding volume based on the assumption of hemispherical shape was $1.75 \times 10^5 \mu\text{m}^3$ ($1.75 \times 10^{-13} \text{m}^3$).

In the photogrammetric approach, we used a closed mesh of the wireframe 3D model (Fig. 7b). We calibrated the model by setting a scale bar representing the diameter of the laser pit with the same start and end points used in the SEM micrograph and used the known measurement to set the scale. PhotoScan then used this scale calibration to determine the volume of the closed mesh to be $2.08 \times 10^5 \mu\text{m}^3$ ($2.08 \times 10^{-13} \text{m}^3$).

The volume determined by the 3D model was 18% greater than the volume calculated by approximating a regular shape. This can be expected as the modeled shape takes into account the contribution to the volume of irregular features.

4. DISCUSSION

4.1 Image Acquisition Parameters

For successful photogrammetry, common features need to be present, detected, and successfully matched in multiple micrographs from different angles around the sample. In addition to requiring focus to be set correctly, due to algorithmic limitations, features cannot be matched reliably when the viewpoint changes too much (i.e. there is too much angular difference between images). Therefore, to allow successful and robust feature matching, a small angle of rotation between micrographs is required resulting in significant overlap of images.

For Method 2, results suggested that a rotational increment of 5° through 360° was required for accurate reconstruction of a 3D model. Greater increment angles of 10° , 15° , and 20° were also tested by eliminating intermediate micrographs. For example, to create a 10° increment dataset, every second image was removed that the remaining images were processed. As expected, higher intervals between micrographs resulted in failed models due to a lack of overlap between successive images. In general, the more images used in photogrammetric reconstruction, the more detailed the resultant model was. Although Method 2

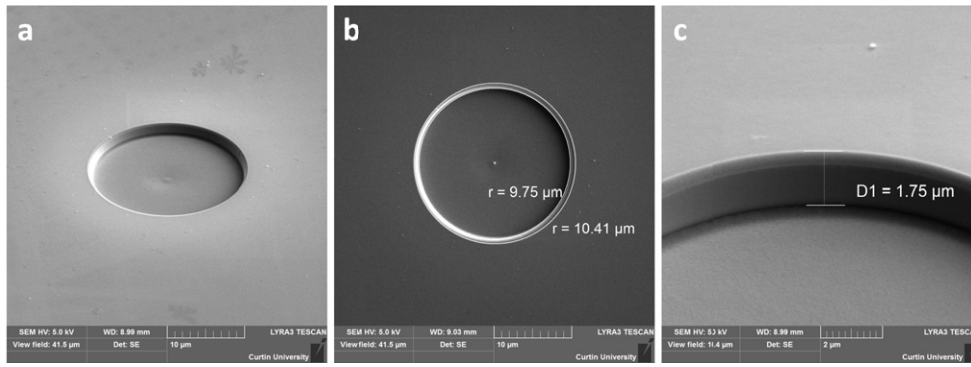


Figure 6. Synthetic laser pit in silicon. (a) Micrograph of the focused ion beam milled pit, (b) annotated radius measurements with an average of $10.08 \mu\text{m}$, and (c) depth measurement of $1.75 \mu\text{m}$.

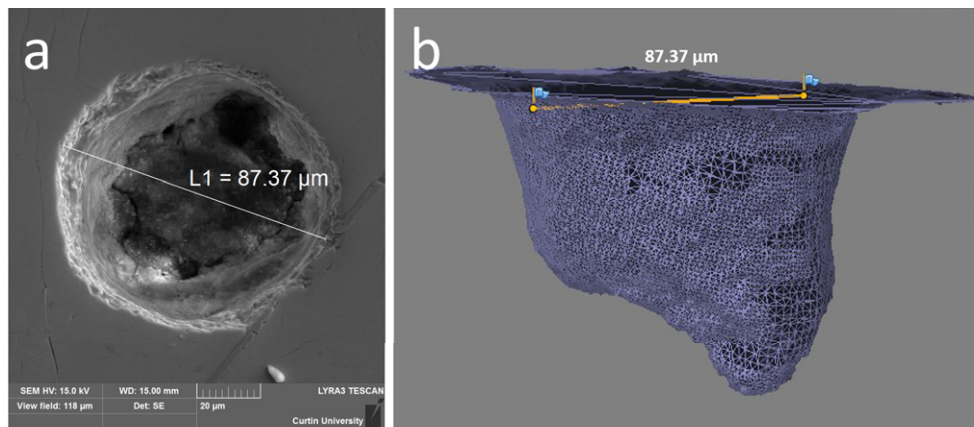


Figure 7. (a) Irregular laser pit micrograph with annotated diameter reading of $87.37 \mu\text{m}$, as shown in blue. (b) Wireframe model of the irregular laser pit with scale bar set to the same length as in (a). This reference value is used by PhotoScan to calculate the volume of the wireframe mesh.

produced successful models, the image acquisition process is slow due to the manual stage rotation in our experiment.

For both Method 1 and Method 2, the accuracy of the 3D reconstruction by photogrammetry relied on the features of the sample, and the quantity and resolution of the micrographs. Experiments conducted with other samples including a screw, textured metal surface, synthetic laser ablation pit on silicon revealed that samples without remarkable features, such as those with flat surfaces or too symmetrical, were not suitable for 3D reconstruction with photogrammetry. Instrument specific software may be obtained to automate stage manipulations such as stage tilt and stage rotation.

Other approaches share consistent findings that successful data collection is sample and instrument specific. Stage rotation for the successful reconstruction in these approaches included Gontard et al. [23] who reconstructed a 3D model of a $\text{LiTi}_2(\text{PO}_4)_3$ particle with 20° stage rotation through 360° around the sample under two stage tilt values, producing 36 micrographs; Eulitz and Reiss [10] reconstructed a rabbit kidney structure using a 40-micrograph dataset taken with a 9° increment stage rotation; and Amish et al. [8] required a

4° increment stage rotation for the reconstruction of an Ebola virus infected cell.

The image acquisition parameters for accurate 3D reconstruction considered in this study are summarized in Table III.

4.2 Volume Analysis using Photogrammetry

The photogrammetric volume measurement technique presented here has advantages including its non-destructive nature, minimal sample preparation time, automated workflow, time and computation efficiency, simple mathematical modeling, and suitable results.

When using photogrammetry for volume analysis, the quality of the reconstruction directly affects the accuracy of the volume measurements. This is evident when attempting to conduct volumetric analysis of samples of irregular shape. In such cases generating an accurate 3D model using photogrammetry is less likely as accurate data acquisition is reduced. For instance, irregular samples such as textured laser pits may suffer from failed models or overhangs, where the surface of the sample correctly captured in the model. Furthermore, features not visible in at least two images will not be correctly stitched resulting in failed models.

Table III. Summary of general operating parameters required for successful micrograph acquisition, including respective values and comments to consider when creating a data collection of SEM micrographs for 3D reconstruction with PhotoScan. Accelerating voltage, scan speed, and working distance are sample dependant and not specific to obtaining good photogrammetric results.

	Parameter	Recommended values	Comments
Required for photogrammetry	Detector	Off-axis SE	On-axis SE and off-axis BSE also performed good results; detector type may vary with micrograph's quality displayed on SEM screen.
	Fixed stage tilt	45°	Recommended tilt for stage rotation in a fixed stage tilt protocol.
	Auto stage tilt range	-15° to +35°	Minimum recommended for an automatic stage tilt protocol (2.5° increment).
		-25° to +70°	Wider automatic stage tilt tested (5° increment), however, requires high values of WD.
	Tilt increment	2.5°	For a 50° range of automatic stage tilt.
	Rotation increment	5°	For higher ranges of automatic stage tilt (> 50°) and for stage rotation (360°) in a fixed stage tilt protocol.
Required for micrograph collection (apart from photogrammetry)	Accelerating voltage (AccV)	5–15 kV	Lower values recommended for biological samples; AccV values should not exceed 15 kV to focus on to acquire topographical information.
	Scan speed	4 s/frame (3.2 μs/pix)	Minimum recommended for less 3D-detail samples.
		43 s/frame (32 μs/pix)	Recommended for general acquisition.
	Working distance (WD)	8–25 mm	Low values recommended for smaller samples; higher WD values are necessary for higher stage tilt values (> 45°).
	Column settings	DEPTH mode	Suggested to maximize depth of focus on image.

The basic approach of approximating the shape and calculating the volume of an irregular shaped object is subject to a high degree of error. Photogrammetry is a promising technique for volume measurement from SEM micrographs for irregular shaped objects. A comparative experiment of calculated volume to model derived volume was attempted in this study though the reconstruction failed due to the lack of unique features between images as identified by PhotoScan. Although not considered in this study, textural features could be added to the surface by depositing nanoparticles; a technique used in transmission electron microscopy (TEM) tomography.

5. CONCLUSIONS

In this contribution, we presented two methods for SEM image acquisition for photogrammetric analysis of microscopic samples and discuss the relative merits of using the technique for volume calculations. Results show that data collection routines suitable for 3D reconstruction is sample dependent, with manual stage rotation in a fixed stage tilt acquisition more suitable for samples with elevated shape, while an automatic stage tilt method is more suitable for concave samples. Furthermore, imaging conditions such as detector type, working distance, accelerating voltage, and scan speed are shown to be dependent on sample type. Our results demonstrate that the photogrammetric approach requires micrographs to have many features and therefore is more successful for irregular over smooth shapes.

When considering irregular shaped objects, volume analysis using 3D models generated by photogrammetry are expected to be more accurate than approximated shape calculations 2D imaging. Although there are other techniques available for volume measurements, the convenience and efficiencies from extracting accurate figures from SEM micrographs makes the photogrammetry approach attractive.

ACKNOWLEDGMENT

This project was supported by the Curtin University HIVE summer research internship program.

REFERENCES

- W. Zhou, R. Apkarian, Z. L. Wang, and D. Joy, *Scanning Microscopy for Nanotechnology* (Springer, Berlin, New York, 2006), pp. 1–40.
- D. Ze-Jun and R. Shimizu, *J. Microscopy* **154**, 193–207 (1989).
- A. P. Tafti, A. B. Kirkpatrick, Z. Alavi, H. A. Owen, and Z. Yu, "Recent advances in 3D SEM surface reconstruction," *Micron* **78**, 54–66 (2015).
- A. Arman, Ş. Tãlu, C. Luna, A. Ahmadpourian, M. Naseri, and M. Molamohammadi, "Micromorphology characterization of copper thin films by AFM and fractal analysis," *J. Mater. Sci. Mater. Electronics* **26**, 9630–9639 (2015).
- A. Daud, G. Gray, C. D. Lynch, N. H. F. Wilson, and I. R. Blum, "A randomised controlled study on the use of finishing and polishing systems on different resin composites using 3D contact optical profilometry and scanning electron microscopy," *J. Dentistry* **71**, 25–30 (2018).
- M. Hemmleb, D. Bettge, I. Driehorst, and D. Berger, "3D surface reconstruction with segmented BSE detector: New improvements and application for fracture analysis in SEM," *European Microscopy Congress: Proceedings* (Wiley Online Library, New York, 2016).

- ⁷ R. Zhang, P.-S. Tsai, J. E. Cryer, and M. Shah, *IEEE Trans. Pattern Anal. Mach. Intell.* **21**, 690–706 (1999).
- ⁸ T. Amish, B. T. Hansen, and E. R. Fischer, *Microsc. Microanal.* **22**, 1144–1145 (2016).
- ⁹ A. D. Ball, P. A. Job, and A. E. Walker, *J. Microscopy* **267**, 214–226 (2017).
- ¹⁰ M. Eulitz and G. Reiss, *J. Struct. Biol.* **191**, 190–196 (2015).
- ¹¹ F.-X. Masson, G. Beaudoin, and D. Laurendeau, “Quantification of the morphology of gold grains in 3D using X-ray microscopy and SEM photogrammetry,” *J. Sedimentary Res.* **90**, 286–296 (2020).
- ¹² J. Fryer, H. Mitchell, and J. H. Chandler, *Applications of 3D Measurement from Images* (Whittles, Dunbeath, Caithness, Scotland, 2007), p. 304.
- ¹³ T. Luhmann, S. Robson, S. Kyle, and I. Harley, *Close Range Photogrammetry Principles, Methods and Applications* (Whittles Publishing, Scotland, UK, 2006).
- ¹⁴ M. Kasser and Y. Egels, *Digital Photogrammetry* (Taylor & Francis, London, 2002).
- ¹⁵ A. Woods, P. Helmholz, A. Bickers, and J. Hollick, *From Great Depths The Wrecks of HMAS Sydney II and HSK Kormoran* (UWA Publishing, Perth, Western Australia, 2016), pp. 255–277.
- ¹⁶ J. J. Medina, J. M. Maley, S. Sannapareddy, N. N. Medina, C. M. Gilman, and J. E. McCormack, “A rapid and cost-effective pipeline for digitization of museum specimens with 3D photogrammetry,” *PLoS One* **15**, e0236417 (2020).
- ¹⁷ G. Barbieri and F. P. da Silva, “Acquisition of 3D models with submillimeter-sized features from SEM images by use of photogrammetry: A dimensional comparison to microtomography,” *Micron* **121**, 26–32 (2019).
- ¹⁸ A. D. Ball, P. A. Job, and A. E. Walker, “SEM-microphotogrammetry, a new take on an old method for generating high-resolution 3D models from SEM images,” *J. Microscopy* **267**, 214–226 (2017).
- ¹⁹ J. Pickering, W. Matthews, E. Enkelmann, B. Guest, C. Sykes, and B. M. Koblinger, “Laser ablation (U-Th-Sm)/He dating of detrital apatite,” *Chem. Geology* **548**, 119683 (2020).
- ²⁰ M. Khokhlov, A. Fischer, and D. Rittel, *Experimental Mech.* **52**, 975–991 (2012).
- ²¹ A. P. Tafti, J. D. Holz, A. Baghaie, H. A. Owen, M. M. He, and Z. Yu, *Micron* **87**, 33–45 (2016).
- ²² F. Glon, O. Flys, P.-J. Lööf, and B.-G. Rosén, *J. Phys.* **483**, 012026 (2014).
- ²³ L. C. Gontard, R. Schierholz, S. Yu, J. Cintas, and R. E. Dunin-Borkowski, *Ultramicroscopy* **169**, 80–88 (2016).
- ²⁴ P. Kozikowski, “Extracting three-dimensional information from SEM images by means of photogrammetry,” *Micron* **134**, 102873 (2020).
- ²⁵ A. Gruen, “Development and status of image matching in photogrammetry,” *The Photogrammetric Record* **27**, 36–57 (2012).